

Choice overload reduces neural signatures of choice set value in dorsal striatum and anterior cingulate cortex

Elena Reutskaja^{1,8}, Axel Lindner^{2,3,4,8*}, Rosemarie Nagel⁵, Richard A. Andersen^{4,6}
and Colin F. Camerer⁷

Modern societies offer a large variety of choices^{1,2}, which is generally thought to be valuable³⁻⁷. But having too much choice can be detrimental^{1-3,8-11} if the costs of choice outweigh its benefits due to ‘choice overload’¹²⁻¹⁴. Current explanatory models of choice overload mainly derive from behavioural studies^{13,14}. A neuroscientific investigation could further inform these models by revealing the covert mental processes during decision-making. We explored choice overload using functional magnetic resonance imaging while subjects were either choosing from varying-sized choice sets or were browsing them. When choosing from sets of 6, 12 or 24 items, functional magnetic resonance imaging activity in the striatum and anterior cingulate cortex resembled an inverted U-shaped function of choice set size. Activity was highest for 12-item sets, which were perceived as having ‘the right amount’ of options and was lower for 6-item and 24-item sets, which were perceived as ‘too small’ and ‘too large’, respectively. Enhancing choice set value by adding a dominant option led to an overall increase of activity. When subjects were browsing, the decision costs were diminished and the inverted U-shaped activity patterns vanished. Activity in the striatum and anterior cingulate reflects choice set value and can serve as neural indicator of choice overload.

In many modern economies consumers have a dizzying variety of choices, even for simple goods like bottled water. A typical US supermarket can carry more than 30,000 items, including 285 kinds of cookies and 275 types of cereal¹. For important lifetime choices, such as decisions about retirement investment, one can be faced with dozens or hundreds of options, with serious consequences if decision making is postponed or avoided entirely².

Is having that much choice good or bad? In the simplest economic theories, more choice is never worse because effort cost is neglected. In that case, the value of a choice set is equal to the value of its most-preferred item, which never decreases as the number of choice options goes up. From a social point of view, larger choice sets are better because they can satisfy a variety of different individual preferences. People also appear to be attracted by having more choices³. Having more choices is also associated with a stronger experience of freedom of choice^{4,5}, and

induces feelings of autonomy and self-control, facilitating intrinsic motivation^{6,7}.

The increased value of having more choice of course ignores costs that can likewise increase with choice set size, such as choice-related information processing, the fear of regret from mistakenly passing up an ideal choice⁸, discomfort due to uncertainty about preferences, lack of expertise, making trade-offs, and so on⁹. In addition, when faced with too many unfamiliar choices, consumers³ and workers² sometimes postpone decisions, which can in itself be a poor choice, and subjects are more likely to change their initial decision¹⁰. These phenomena together are often taken as evidence for human ‘choice overload’¹¹.

Some behavioural studies try to directly measure the trade-off between the benefits and costs of choosing, as a function of choice set size. These studies generally show that consumers prefer choice sets containing 8 to 15 alternatives over choice sets that contain only 2 to 6 items, which is perceived as ‘too few’. Yet, if the number of choice alternatives increases beyond 15, choice sets are mostly perceived as ‘too large’^{1,3,12,13,15}.

The results of studies on choice overload can be qualitatively captured by a simple explanatory model with two components (Fig. 1a)^{13,14}. One component reflects the costs of choosing (U_c ; for example, cognitive load, time), which are assumed to increase with the size of the choice set, S . The second component captures the benefits of choosing (U_b ; for example, the feeling of ‘freedom of choice’, the probability of finding an ideal choice), which also increase with S but at a lower rate than costs increase. If benefits increase slower than costs increase¹⁶, the net value of the choice set (the set value, $U_o = U_b - U_c$) will have an inverted U shape. This set value represents the integrated subjective ‘benefits’ of choosing net of the costs experienced during choosing from the set, and is reflected in a feeling of whether one felt deprived of choice, ‘just right’ about the choice, or overwhelmed with the choice options faced. We conceive of this choice set value as also serving as a motivational signal that generally maintains cognitive and behavioural engagement in decision making but which—in case of choice overload—becomes demotivating.

It is important to note, however, that larger choice sets do not automatically lead to choice overload. For instance, Iyengar and

¹Marketing Department, IESE Business School, Barcelona, Spain. ²Department of Psychiatry and Psychotherapy, University Hospital Tübingen, Tübingen, Germany. ³Department of Cognitive Neurology, Hertie-Institute for Clinical Brain Research, Tübingen, Germany. ⁴Division of Biology and Biological Engineering, California Institute of Technology, Pasadena, CA, USA. ⁵Institució Catalana de Recerca i Estudis Avançats, Barcelona Graduate School of Economics, Department of Economics and Business, Universitat Pompeu Fabra, Barcelona, Spain. ⁶The Tianqiao and Chrissy Chen Brain-Machine Interface Center, California Institute of Technology, Pasadena, CA, USA. ⁷Division of the Humanities and Social Sciences and Computation and Neural Systems, California Institute of Technology, Pasadena, CA, USA. ⁸These authors contributed equally: Elena Reutskaja, Axel Lindner.

*e-mail: a.lindner@medizin.uni-tuebingen.de

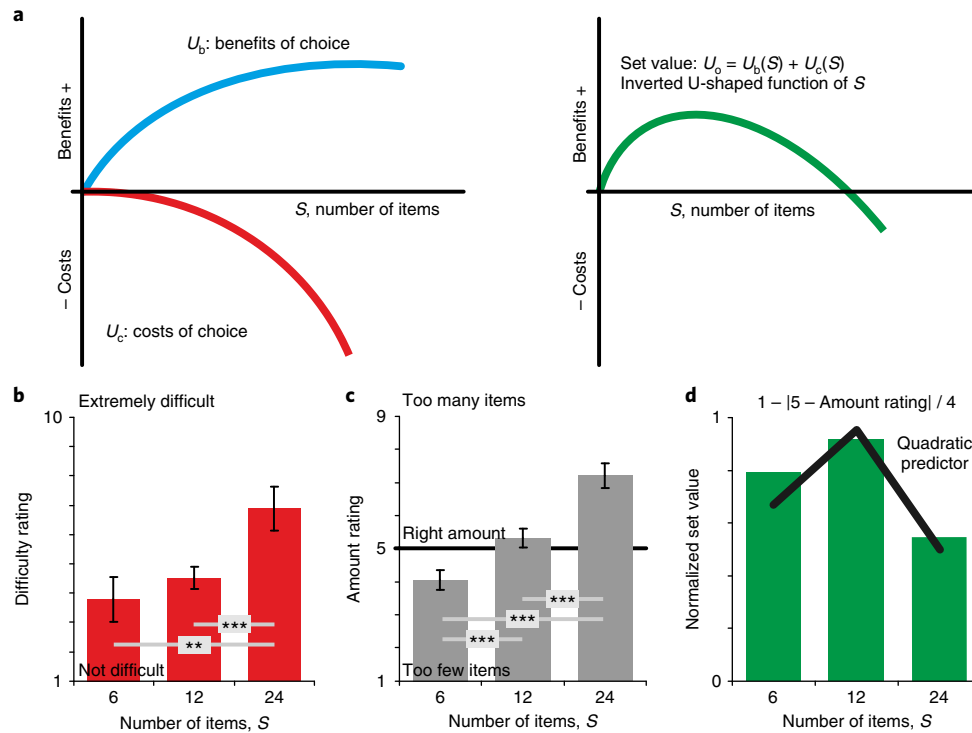


Fig. 1 | Choice set value. **a**, This model describes the satisfaction with a choice set (U_o), here referred to as choice set value, as the net benefit of choosing. U_o reflects the difference between the benefits (U_b) and the costs (U_c) of choosing, which increase with the choice set size S . Because costs increase faster than benefits, the choice set value is described by an inverted U-shaped function of S . **b**, Difficulty rating, showing subjects' average perceived choice difficulty as a function of choice set size ($N=19$; data presented as mean and 95% CI; between subject-variance was removed according to the procedures specified in ref. ⁶⁷). Differences in ratings between sets were assessed by a one-way repeated measures ANOVA (see main text) and pairwise post hoc comparisons (P values were Bonferroni-corrected for multiple comparisons; 6 versus 12: $t(18)=1.546$, $P=0.418$, g_1 (95% CI)=0.355 (-0.114, 0.814); 6 versus 24: $t(18)=4.147$, $^{**}P=0.002$, g_1 (95% CI)=0.951 (0.397, 1.488); 12 versus 24: $t(18)=5.077$, $^{***}P<0.001$, g_1 (95% CI)=1.165 (0.568, 1.742)). **c**, Amount rating assessing subjects' experience of the choice process ($N=19$; data presented as mean and 95% CI). This was significantly influenced by set size (one-way repeated measures ANOVA with factor set size (see main text) and pairwise post hoc comparisons; $t(18)=5.555$, $^{***}P<0.001$, g_1 (95% CI)=1.274 (0.654, 1.875); 6 versus 24: $t(18)=10.240$, $^{***}P<0.001$, g_1 (95% CI)=2.349 (1.457, 3.224); 12 versus 24: $t(18)=6.215$, $^{***}P<0.001$, g_1 (95% CI)=1.426 (0.771, 2.061)). **d**, Normalized group estimate of subjects' choice set value. This estimate was derived from the average amount rating in **c** and according to the formula shown. A value of '1' characterizes a set size, which is perceived as optimal, while '0' identifies least optimal set sizes. This normalized estimate of set value resembles an inverted U-shaped profile as a function of S , as is suggested by the model in **a**. Normalized set value is well described by the quadratic predictor used for fMRI analyses (black line is a linear fit to the data).

Lepper³ have demonstrated that prior to choice, large sets are often considered to be more attractive than smaller sets, but they become less motivating during the process of choosing, once decision costs are experienced. In this Article we focus on this latter situation: we study the value of the choice set once the benefits and costs of choosing are experienced. Choice overload is also not experienced in all choice contexts¹⁷. A recent meta-analysis identified four relevant factors that moderate the impact of choice set size on choice overload¹¹. Choice overload increases with (1) decision task difficulty (for example, time pressure), (2) choice set complexity (for example, due to the absence of a clearly preferred, dominant option¹⁸) and (3) preference uncertainty (for example, choice made by experts versus non-experts). Finally, set value is also modulated by (4) decision goals (for example, 'choosing' versus 'browsing'^{19,20}).

Explanatory models of choice overload should further detail the benefits and costs of choice, and their modulation through these extrinsic ((1) and (2)) and intrinsic ((3) and (4)) factors as they vary across individuals and choice contexts. A neuroscientific investigation of the phenomenon of choice overload might help to further inform these models, which thus far build only on studies engaging behavioural measures or self-reports. Neural observation could help in building more precise models of choice overload by revealing

covert processes during decision making, and by possibly identifying the 'bottlenecks' that reduce the value of large choice sets.

Here we report an initial approach, using functional magnetic resonance imaging (fMRI) to identify brain areas that represent the value of a set as a whole. We hypothesized that areas associated with set value would exhibit an inverted U-shaped activity profile as a function of set size S , and that the inverted U shape is further modulated by choice set complexity and decision intent.

We hypothesized that the striatum and the anterior cingulate cortex (ACC) are likely candidates for coding choice set value. There is evidence that both areas represent value signals net of costs²¹ and are thought to motivate engagement in executive control and choice behaviour^{22,23}. Yet, it is an open question whether these (or any other) brain areas represent choice set value, which is a representation that goes beyond the evaluation of individual items within a set (or the value of the chosen item).

We further hypothesized that the increasing costs of choosing from large sets would be reflected in activity in task-related areas engaged in visual and sensorimotor processing, and by more frequent eye saccades used to visually inspect available choices^{15,24–27}.

Next we demonstrate that activity in the striatum and ACC did initially exhibit an inverted U-shaped activity profile as a function

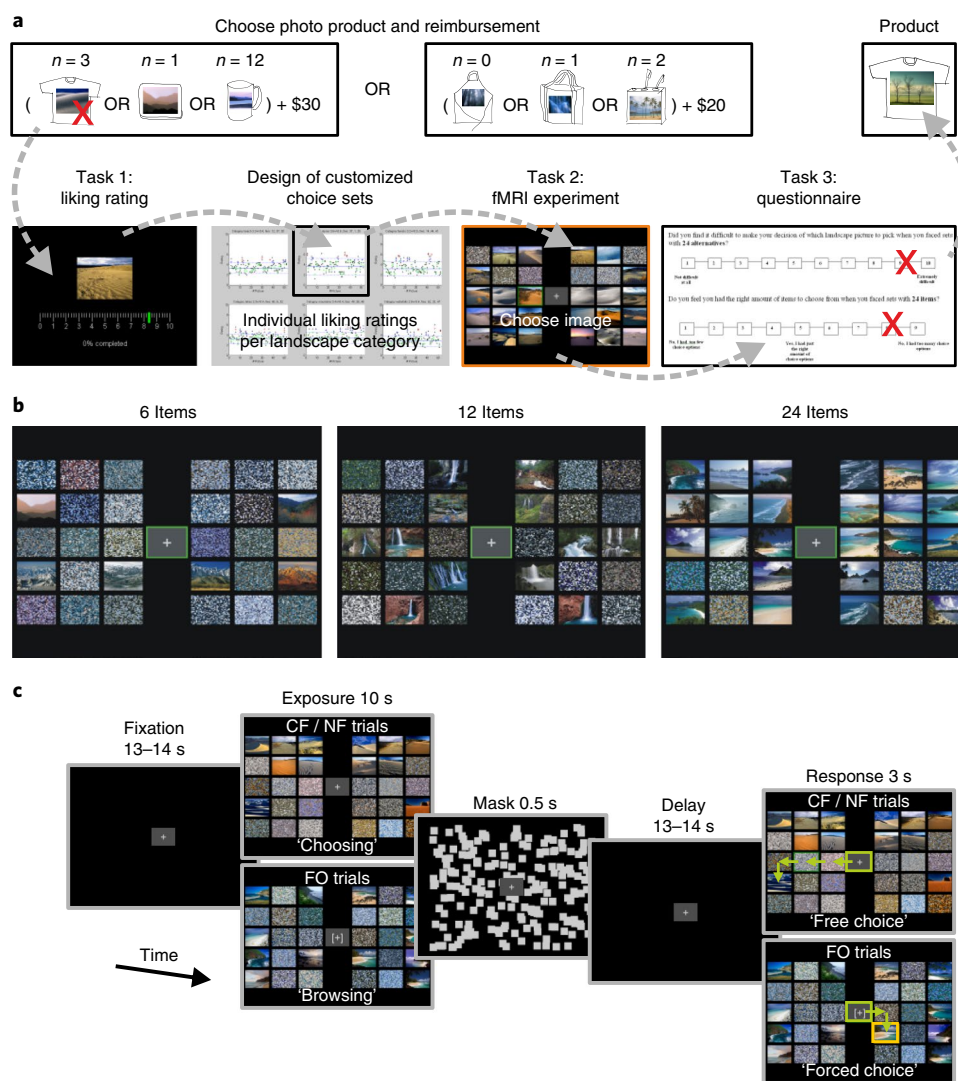


Fig. 2 | Experimental design. **a**, Overview of the different tasks performed during the experiment. **b**, Exemplary choice sets, reflecting sets of small, medium and large size ($S = 6, 12$ or 24 , respectively). The sets were created using images from terragalleria.com with permission from the website. **c**, Timeline of the choice task performed during fMRI is shown in **c**. Subjects inspected the choice items during ‘exposure’ and manually reported their choice during ‘response’.

of set size S that, in addition, was modulated by choice set complexity and by decision intent. This inverted U-shaped profile vanished during later stages of a trial when decision-related fMRI activity instead reflected the value of the chosen item.

In our study subjects had to choose pictures from sets of unfamiliar landscape images. The image chosen by the subjects in one randomly selected trial was later printed on a product of their choice (for example, a t-shirt or a mug) and had to be picked up by them (Fig. 2a). Hence, our fMRI experiment mimicked a natural choice setting with actual consequences, in which subjects choose from sets containing different number of choice alternatives S .

Our study was completed by $N = 19$ subjects, which performed three subsequent tasks: (1) A liking rating assessing the desirability of the available landscape photographs; (2) an fMRI experiment engaging a choice task in which the subject needed to select an image in different sized choice sets; (3) a questionnaire task, evaluating one’s choice experience in the choice task (2) (Fig. 2a).

In task 1, which was performed before fMRI scanning, subjects rated how much they wanted each picture to be printed on the product of their choice (procedure adopted from ref. ¹⁵). They rated 312

pictures (52 pictures $\times 6$ landscape categories) twice. The final rating of each image was determined by the average rating calculated across the two rounds. This allowed us to create customized choice sets for each individual in a way that accounted for the subjective value of each image within a set.

In task 2, we scanned brain activity while subjects were choosing their preferred picture from the customized choice sets consisting of either $S = 6, 12$ or 24 pictures of the same landscape category (Fig. 2b). These three different set sizes S were selected based on prior research^{2,3,10–13,15} to create sets with high choice set value (that is, having ‘just the right amount of alternatives’; $S = 12$) and with lower choice set value (that is, carrying ‘too few’ ($S = 6$) or ‘too many’ ($S = 24$) alternatives, respectively). Any brain area that would display activity reflecting an inverted U-shaped pattern as a function of S (Fig. 1a) would be considered a candidate region potentially representing choice set value.

To further clarify whether these candidate areas do reflect choice set value, we also varied whether a highly rated ‘clear favourite’ item (CF) was available in a set or not (‘no favourite’, NF) (Supplementary Fig. 1c,d). As mentioned above, choice set processing costs typically

decrease when a highly preferred dominant option is present^{10,18}. Therefore, we expected a corresponding increase in set value related brain activity in CF as compared to NF. Finally, these free choice trials were contrasted with ‘forced choice’ (FO) trials. FO trials mimicked the NF condition except that subjects made an involuntary choice of a highly valued item, dictated by a computer. This manipulation should alter subjects’ decision intent from ‘choosing’ (in free choice trials) to ‘browsing’ (in forced choice trials), thereby diminishing the costs of choosing and choice overload^{19,20}. Accordingly, set value related brain activity in FO trials should uncover only the benefits of larger choice sets and thus offset the inverted U-shaped activity profile discussed earlier (see U_b in Fig. 1a).

All conditions had an equal share and were presented randomly interleaved (72 trials total, split into 4 runs). Each trial was composed of an initial baseline epoch with central fixation (13–14 s), a fixed 10 s exposure to the choice set, a 0.5 s mask to reduce after-image contrast, a 13–14 s delay with central fixation, and a brief 3 s response stage displaying the choice set a second time (Fig. 2c). During the response stage subjects had to guide a cursor to the selected image to indicate their decision. Subjects’ eye movements were also recorded throughout the fMRI experiment. Our measures of both eye movements and brain activity are chiefly reported for the exposure period in which subjects inspected the choice sets. This is because we were particularly interested in the processes that contribute to the evaluation of a choice set and their neural implementation. The 10 s duration of the exposure period was chosen based on previous research¹⁵ and a pilot experiment in an attempt to ensure that (1) subjects are able to make high-quality decisions and (2) they make use of the full length of the exposure period to inform their decisions. The delay served to allow a separation of choice set related decision activity during the exposure stage, from memory maintenance, motor preparation and action execution in the later response stage²⁸.

In task 3, which was performed after scanning, subjects had to answer a questionnaire (Fig. 2a). Subjects had to rate the difficulty of choosing from each set size on a 10-point scale from 1 (‘Not difficult at all’) to 10 (‘Extremely difficult’; Fig. 1b). They next had to report whether the choice sets contained the ‘right number of items’ on a 9-point scale, with 5 meaning ‘Yes, I had just the right amount of choice options’, and with lower numbers indicating too few options and higher numbers indicating too many options (Fig. 1c) (measure adopted from previous research³). Based on the across-subject average of this estimate we further derived the normalized set value as

$$1 - |5 - \text{Average amount rating}| / 4$$

In other words, a set size is perceived as optimal if this index is 1 while a set size is perceived as least optimal if this index is 0 (Fig. 1d). See Methods and Supplementary Methods for further details on the design of the study.

As we hypothesized, perceived difficulty of choosing increased with S (Fig. 1b; one-way repeated measures analysis of variance (ANOVA) with factor set size: $F(1,376, 24.771) =$, $P < 0.001$, η_p^2 (95% confidence interval (CI)) = 0.466 (0.1973, 0.6122)). Set size also had a significant influence on the amount rating (one-way repeated measures ANOVA with factor set size: $F(2,36) = 63.220$, $P < 0.001$, η_p^2 (95% CI) = 0.778 (0.6449, 0.8317)). Subjects rated the 12-item set as having just ‘the right number of options’ while sets with 6 and 24 alternatives were perceived as having ‘too few’ and ‘too many’ items, respectively (Fig. 1c). Accordingly, the group estimate of normalized set value (Fig. 1d) was highest for choice sets of intermediate size and lower for smaller and larger sets, showing the predicted inverted U-shaped function (Fig. 1a,d).

Next we show that reaction times demonstrate that the exposure period and the delay stage are sufficiently long to allow subjects to make a decision in all free choice trials. If subjects indeed settled on

one specific item in a set during the exposure period, then preparing the motor response required to choose was beneficial because of the brief 3 s duration of the response stage. We defined the reaction time (RT) as the amount of time elapsed from the appearance of the response screen until a subject first started to move the cursor towards the chosen item. If choices are made during the exposure period and held in memory, then RTs should be longer in the forced choice condition (FO) than in the matched free choice condition (NF)[29], as response preplanning was not possible in FO (because the item the subject was instructed to choose was only indicated during the response phase). Indeed, RTs were significantly shorter when subjects were freely choosing (NF; mean (M) = 562 ms \pm 53 ms (CI)) than during forced choice (FO; $M = 740$ ms \pm 43 ms (CI)); two-way repeated measures ANOVA with factors condition (NF versus FO) and set size (S); condition: $F(1,18) = 50.720$, $P < 0.001$, η_p^2 (95% CI) = 0.738 (0.505, 0.822)). In addition, RTs in both conditions did not exhibit any variation as a function of choice set size S (set size: $F(2,36) = 1.207$, $P = 0.311$, η_p^2 (95% CI) = 0.063 (0.000, 0.185); interaction: $F(2,36) = 0.372$, $P = 0.692$, η_p^2 (95% CI) = 0.020 (0.000, 0.101); Fig. 3a). Nor did RTs differ between the two free choice conditions (two-way repeated measures ANOVA with factors condition (CF versus NF) and set size (S); condition: $F(1,18) = 1.376$, $P = 0.256$, η_p^2 (95% CI) = 0.071 (0.000, 0.286); set size: $F(1,383, 24.886) = 0.603$, $P = 0.496$, η_p^2 (95% CI) = 0.0324 (0.000, 0.177); interaction: $F(2,36) = 1.532$, $P = 0.230$, η_p^2 (95% CI) = 0.078 (0.000, 0.208)). Hence, response preparation was identical in CF and NF and also did not vary with set size S (Fig. 3a).

Eye movement recordings demonstrate that the number of saccadic eye movements was influenced by the size of the choice set S . The number of saccades per second increased with S during the exposure period of all conditions (Fig. 3b), while average saccade amplitudes decreased (Fig. 3c). Accordingly, a significant influence of choice set size S was revealed by separate two-way repeated measures ANOVAs (factors set size and condition (CF versus NF or NF versus FO)) for both saccade frequency (set size (CF versus NF): $F(1,464, 26.353) = 96.812$, $P < 0.001$, η_p^2 (95% CI) = 0.843 (0.723, 0.886); set size (NF versus FO): $F(2,36) = 74.421$, $P < 0.001$, η_p^2 (95% CI) = 0.805 (0.686, 0.852)) and saccade amplitude (set size (CF versus NF): $F(2,36) = 20.650$, $P < 0.001$, η_p^2 (95% CI) = 0.534 (0.314, 0.643); set size (NF versus FO): $F(1,523, 27.418) = 11.239$, $P < 0.001$, η_p^2 (95% CI) = 0.384 (0.131, 0.541)). Between conditions CF and NF the number and amplitude of saccades was indistinguishable (frequency: $F(1,18) = 2.721$, $P = 0.116$, η_p^2 (95% CI) = 0.131 (0.000, 0.357); amplitude: $F(1, 18) = 0.666$, $P = 0.425$, η_p^2 (95% CI) = 0.036 (0.000, 0.222)) and their modulation with S was similar in both conditions (interaction frequency: $F(2,36) = 1.507$, $P = 0.235$, η_p^2 (95% CI) = 0.077 (0.000, 0.207); interaction amplitude: $F(2,36) = 1.202$, $P = 0.312$, η_p^2 (95% CI) = 0.063 (0.000, 0.185)). The overall number of saccades was, however, smaller during ‘browsing’ (FO; $M = 1.01$ saccades per second \pm 0.14 (95% CI)) compared with ‘choosing’ (NF; $M = 1.24$ saccades per second \pm 0.12 (95% CI)); condition: $F(1,18) = 20.616$, $P < 0.001$, η_p^2 (95% CI) = 0.534 (0.229, 0.682)) and the increase with S was smaller in FO than in NF (interaction: $F(2,36) = 9.985$, $P < 0.001$, η_p^2 (95% CI) = 0.357 (0.131, 0.497)). Average saccade amplitude did not differ between FO and NF (condition: $F(1,18) = 2.053$, $P = 0.169$, η_p^2 (95% CI) = 0.102 (0.000, 0.325)), but did decrease more strongly as a function of set size S in NF than in FO (interaction: $F(2,36) = 5.283$, $P = 0.010$, η_p^2 (95% CI) = 0.227 (0.036, 0.378)). Given that increases in saccade frequency rather than in saccade amplitude demand greater neural resources³⁰, these results imply that the motor costs and attentional demands increase with set size, and are higher in the CF and NF conditions requiring a choice than in FO. An additional time-resolved analysis of saccade frequency during the exposure period suggests that subjects made use of the full length of this period to inspect the choice sets in all conditions (Supplementary Fig. 2). Importantly, these data (and Fig. 3b)

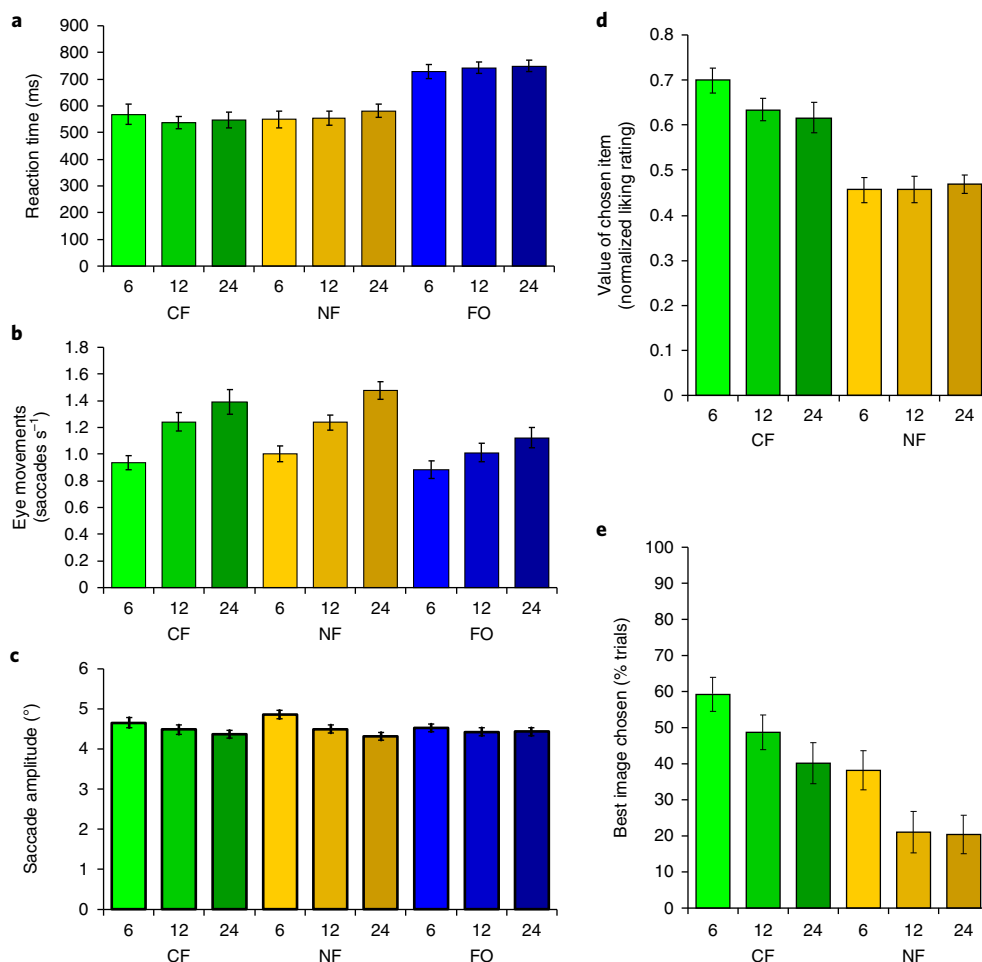


Fig. 3 | Behavioural performance. **a**, Average reaction times for initiating cursor movements towards the chosen image relative to the onset of the response phase. Reaction times are shown for each experimental condition (CF, NF and FO) and each choice set size ($S=6, 12$ and 24). **b**, Mean number of saccades per second during the exposure phase of the fMRI task for each condition (CF, NF and FO) and for each set size. **c**, Mean saccade amplitudes during the exposure phase for each condition and for each set size. **d**, Average value of the chosen item in free choice conditions (CF and NF) and for different set sizes. **e**, Average likelihood that the best-rated image was chosen in choice trials (CF and NF), shown separately for different set sizes S . Estimates were calculated across individual subjects' means. $N=19$; error bars denote s.e.

also indicate that subjects 'browsed' the available choice options even in FO trials when there was no need to choose by oneself. This is further supported by self-reports in our questionnaires: most subjects either always (26%) or often (63%) thought about which image they would have selected by themselves in the FO condition. (Two other subjects said they never thought about choosing during FO trials or gave no answer.)

An important behavioural question is how closely liking ratings are associated with the choices subjects made in NF and CF trials. To answer it we assessed the normalized value of the chosen item across trials and conditions according to the following equation (using rating minima and maxima across all images of all trials):

$$\frac{\text{Liking rating of chosen item} - \text{Minimum liking rating}}{\text{Maximum liking rating} - \text{Minimum liking rating}}$$

This normalized value of the chosen item only equals one if the most favourite image of all 312 possible images was selected, and this value equals zero if the least favourite image of all is chosen. Note that all sets for a given condition and subject were created in such a way that differences in their mean liking rating were minimized across the three set sizes (Supplementary Fig. 1a and

Supplementary Methods). The value of the chosen item was significantly higher in CF ($M=0.65 \pm 0.05$ (CI)) than in NF conditions ($M=0.46 \pm 0.05$ (CI)), as would be expected due to the presence of a more highly rated, dominant option in CF (two-way repeated measures ANOVA with factors condition and set size; condition: $F(1,18)=115.707$, $P<0.001$, η_p^2 (95% CI)=0.865 (0.728, 0.908); Fig. 3d). The value of the chosen item decreased with increasing set size (set size: $F(2,36)=4.225$, $P=0.022$, η_p^2 (95% CI)=0.190 (0.016, 0.341)). However, this decrease was only apparent in CF and, accordingly, is reflected by a statistical trend for an interaction of factors condition and set size (interaction: $F(2,36)=3.010$, $P=0.062$, η_p^2 (95% CI)=0.143 (0.000, 0.290)). Note that the lack of a set size effect in the NF condition could be a reflection of the smaller average variability in liking ratings in NF sets (compare Supplementary Fig. 1b,d).

Subjects chose the image with the highest liking rating significantly more in CF ($M=49 \pm 6\%$ (CI)) as compared to NF trials ($M=27 \pm 9\%$ (CI); two-way repeated measures ANOVA with factors condition and set size; condition: $F(1,18)=18.471$, $P<0.001$, η_p^2 (95% CI)=0.506 (0.199, 0.663); Fig. 3e). This suggests that choice was actually easier in CF trials due to the presence of a dominant option; the respective choice set values, encoded neurally, should therefore be higher in CF than in NF trials. Note that in both

free choice conditions the likelihood of selecting the best-rated image decreased significantly with increasing set size S (set size: $F(2,36) = 10.686$, $P < 0.001$, η_p^2 (95% CI) = 0.373 (0.145, 0.511); interaction: $F(2,36) = 0.486$, $P = 0.619$, η_p^2 (95% CI) = 0.026 (0.000, 0.117)). The same qualitative effect held when correcting for choosing favourite items just by guessing; condition: $F(1,18) = 18.828$, $P < 0.001$, η_p^2 (95% CI) = 0.511 (0.204, 0.666); set size: $F(2,26) = 3.334$, $P = 0.047$, η_p^2 (95% CI) = 0.156 (0.001, 0.305); interaction: $F(2,26) = 0.524$, $P = 0.597$, η_p^2 (95% CI) = 0.028 (0.000, 0.122).

Next we searched for regions that exhibit blood-oxygenation-level-dependent (BOLD) signals reflecting choice set value. We applied a whole-brain general linear model (GLM) in which we separately modelled each of our experimental conditions for each of our three main task stages (exposure + mask, delay, response). We included parametric modulators, which captured fMRI-signal modulations that were linearly increasing with S (that is, either reflecting costs or benefits) and that were reflecting an inverted U-shaped function of S (that is, capturing set value). The linear predictor was formed by convolving a canonical fMRI-response function with the normalized set size ($S_{\text{linear}(S)} = (S - S_{\text{mean}}) / S_{\text{mean}}$; with $S_{\text{mean}} = 14$ as the average set size). The inverted U-shaped or quadratic predictor resulted from a convolution with the negative square of normalized set size ($S_{\text{quadratic}(S)} = -S_{\text{linear}(S)}^2$) and was orthogonalized to the linear predictor. This quadratic predictor fits the average estimate of set value (Fig. 1d) and thus is a sensible tool to detect correlated fMRI activity with set value on the group level. The advantage of this approach is that it allows us to independently assess both linear and quadratic signal components associated with set size S (see Supplementary Discussion for a critical assessment of alternative experimental approaches). A parametric modulator was included to capture signal fluctuations that corresponded to the liking rating (desirability) of the chosen item in any given trial. The initial fixation period (13–14 s) served as an implicit baseline for fMRI analyses (Fig. 2c).

fMRI activity increasing linearly with S during the exposure stage of the pooled choice conditions (CF and NF) was exhibited in the left occipital cortex (lingual gyrus (LG) also encroaching fusiform gyrus; inferior occipital gyrus (IOG); middle occipital gyrus, (MOG)), left posterior parietal cortex (superior parietal lobule (SPL)), bilateral dorsal premotor cortex (PMd) and bilateral supplementary motor area (SMA) (red areas in Fig. 4a). Most of these areas have been previously associated with the planning and control of movement (for example, reaches and saccades), the processing of visual scenes, or both^{24–27}.

Areas exhibiting fMRI activity correlated with the quadratic predictor in the pooled choice conditions (CF and NF) during the exposure stage included bilateral ACC, the striatum (bilateral caudate nucleus (CN) and the left putamen (PUT)), left thalamus (Thal), bilateral dorsolateral prefrontal cortex (DLPFC) (middle frontal gyrus (MFG)), bilateral anterior insula (aINS) extending towards the posterior orbitofrontal cortex (POG, also referred to as the lateral orbitofrontal cortex), left ventral and dorsal premotor cortex (PMv and PMd), bilateral posterior parietal cortex (along the posterior part of the intraparietal sulcus (pIPS)) and occipital cortex (left LG, left IOG and right MOG) (green areas in Fig. 4a and Supplementary Table 1). The inverted U-shaped profile of the fMRI responses underlying this correlation is also seen when these areas' beta estimates in CF and NF are plotted as a function of S (see Fig. 4b for a representative subset of regions). Figure 4c shows the respective time courses of fMRI activity in these areas for the pooled choice conditions and as a function of S . Visual inspection of the time courses clearly confirms the inverted U-shaped activity profile throughout the exposure period. Activity in the 12-item set was consistently higher than for 6- and 24-item sets. Interestingly, however, this inverted U-shaped activity profile vanished during the delay and response stages.

Due to their quadratic activity profile, the aforementioned brain areas were considered candidate regions that represent choice set value. Such neural representation of choice set value should also be modulated by choice set complexity and decision intent. To test this assumption, candidate regions were further subjected to region of interest (ROI) analyses (see Methods). Areas encoding choice set value should increase their activity in the presence of a dominant option (CF > NF) (criterion (1), 'choice set complexity'), and show a less quadratic activity profile when shifting subjects' decision intent from 'choosing' (NF) to 'browsing' (FO) (criterion (2), 'decision intent'). We would only consider those candidate areas to reflect choice set value that would survive these former criteria. In addition, we controlled for the simultaneous presence of a positive linear signal component (that is, beta values for the linear predictor are larger than zero) as well as for a positive linear correlation of activity with the number of saccades and with the difficulty rating in free choice conditions (CF and NF; Supplementary Table 1).

Criterion (1): Among our candidate ROIs, beta estimates were significantly higher in CF than in NF sets in bilateral dorsal striatum (PUT/CN), bilateral ACC, left aINS/POG, the left DLPFC (MFG), the left ventral premotor cortex (vPM) and left thalamus. These differences are illustrated in Fig. 4b for left dorsal striatum (PUT/CN) and right ACC, in which the beta estimates were significantly higher whenever a dominant option was present (green bars, CF) as compared to the situation when a dominant option was not present (yellow bars, NF) (also compare the detailed results of the underlying repeated measures ANOVAs with the factors condition (CF versus NF) and set size S (factor of no interest) shown in Supplementary Table 1; see Supplementary Fig. 3a for a depiction of the same qualitative effect in the left MFG).

Criterion (2): Shifting subjects' decision intent from 'choosing' to 'browsing' further abolished the 'quadratic' cost-related signal component in left dorsal striatum and right ACC (that is, the cost-related signal is diminished in NF). Specifically, in Fig. 4b an inverted U-shaped activity profile as a function of S is clearly visible in the left striatum (PUT/CN) during 'choosing' (NF and CF) but not during 'browsing' (FO). Accordingly, the respective quadratic predictors captured significantly less variance in FO compared with NF, as documented in Fig. 4d. The same effect was present in right ACC (Fig. 4d). Similar trends can be observed also for left POG and left MFG (Supplementary Table 1 and Supplementary Fig. 3c). In contrast to the activity in the left dorsal striatum, however, this region in the right ACC further exhibited a positive linear signal component in free choice trials (one-tailed t -test: $t(18) = 2.000$; $P = 0.030$; effect size estimate g_1 (95% CI) = 0.459 (−0.021, 0.927)) and a significant correlation of its activity with subjects' difficulty ratings (linear regression: $F(1,112) = 7.622$, $P = 0.007$, r (95% CI) = 0.252 (0.072, 0.417)) (Supplementary Table 1). This suggests a simultaneous representation of decision costs in this area.

Finally, we compared how normalized set value and the value of the chosen item were represented throughout the different task stages within the latter ROIs (Fig. 4e). We expected that choice set value should primarily be represented during the exposure period of our task (that is, when subjects first face the choice sets), while representations of the value of the chosen item should surface at the later task stages, namely the delay phase, when subjects need to complete and remember their decision, and the response phase. Indeed, the left dorsal striatum and right ACC exhibited a significant quadratic signal component capturing choice set value during the exposure stage only (Fig. 4e; also see Supplementary Fig. 3d for the presence of the same qualitative effect in left POG and left MFG). The value of the chosen item is, instead, only represented during the delay stage in right ACC and during the response stage in left dorsal striatum. Accordingly, an additional repeated measures ANOVA with the factors task stage and GLM regressor (quadratic predictor versus liking rating of the chosen item) revealed a significant interaction for

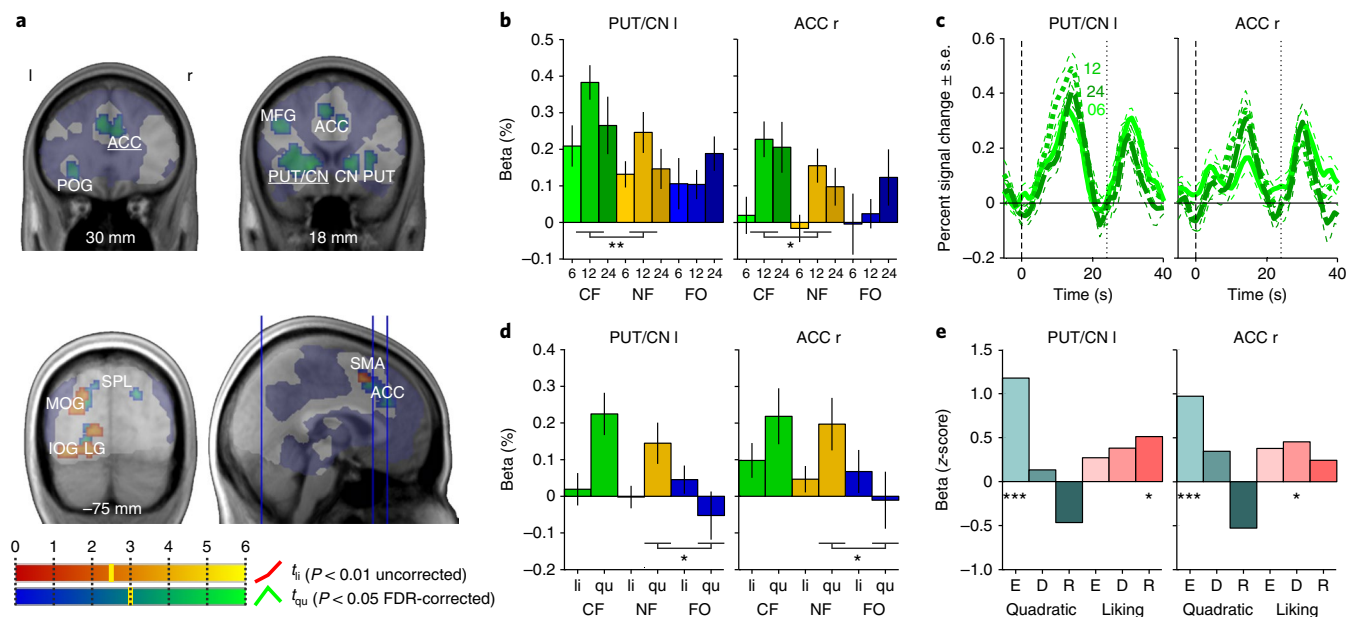


Fig. 4 | Brain areas reflecting choice set value. **a**, Brain areas shown in red to yellow exhibit a linear increase in fMRI activity as a function of S during the exposure stage of the pooled choice trials (CF and NF). Areas shown in blue to green show quadratic, inverted U-shaped fMRI activity profiles. The volume in light grey corresponds to ‘choice-related areas’, activated during the exposure phase of either CF or NF trials. Group analyses were confined to this functional volume of task-related areas. The blue shaded area indicates the remaining image volume, which (1) did not exhibit task-related activity and (2) could be consistently imaged across all of our subjects without signal dropouts. y coordinates are in MNI space. **b–d**, Response profiles of ROIs selected based on quadratic set size function. **b**, Mean beta estimates of choice-related fMRI activity in the exposure phase for each experimental condition as a function of set size S (6, 12 and 24). Error bars denote s.e. Asterisks indicate significant differences in betas between CF and NF, as revealed by a two-way repeated measures ANOVA with the factors condition (PUT/CN I: $F(1,18) = 9.275$, $**P = 0.007$, η^2P (95% CI) = 0.340 (0.188, 0.481); ACC r: $F(1,18) = 6.934$, $*P = 0.017$, η^2P (95% CI) = 0.278 (0.148, 0.409)) and set size (factor of no interest). **c**, fMRI signal time courses corresponding to the ROI analyses in **b**, calculated across the pooled free choice conditions. Separate curves represent choice set sizes. **d**, Mean beta estimates for the linear (li) and quadratic (qu) predictor of each condition during the exposure stage. Any significant reduction of the quadratic signal component in FO compared with NF is highlighted (one-tailed paired t -tests; PUT/CN I: $t(18) = 1.997$; $*P = 0.031$; g_1 (95% CI) = 0.458 (−0.021, 0.926); ACC r: $t(18) = 2.210$; $*P = 0.020$; g_1 (95% CI) = 0.507 (0.022, 0.980)). **e**, Subjects’ z -scored average beta values of the quadratic predictor and the chosen-value (liking) regressor of the pooled free choice conditions, shown separately for each task stage (E, exposure; D, delay; R, response). Beta values significantly larger than 0 are indicated (one-tailed t -tests; $*P < 0.05$, $***P < 0.001$; for detailed statistics see Supplementary Table 2). l and r denote left and right, respectively. $N = 19$.

the dorsal striatum (task stage: $F(1.533, 27.599) = 3.745$, $P = 0.836$, η_p^2 (95% CI) = 0.007 (0.000, 0.091); regressor: effect of no interest; interaction: $F(1.508, 27.142) = 4.770$, $P = 0.025$, η_p^2 (95% CI) = 0.209 (0.016, 0.388)), suggesting a temporally distinct representation of two types of value signal within the dorsal striatum, which shifts from a valuation of the choice set during exposure to a valuation of the chosen item during the response.

Our overall results revealed a neural representation of choice set value in the striatum and the ACC (and potentially in the left DLPFC and in left POG) that is distinct from a valuation of individual items or actions.

The phenomenon of choice overload was first established and explored in psychology, and later in marketing and decision theory^{1–3,10,11,15,18,19}. Many behavioural studies provided support to an explanatory cost–benefit model of choice set value^{9,12–14} that also guided our approach (Fig. 1a). This model hypothesizes an inverted U shape for valuation of choice sets.

Our design specified three sizes of choice set, creating the possibility of detecting the inverted U-shaped relation. When working on these sets, subjects experienced higher processing costs when choosing from larger set sizes. Increased cost was indicated by subjective difficulty ratings (Fig. 1b), increases in the number of eye movement saccades (Fig. 3b), and fMRI signal amplitudes in visual and sensorimotor areas (Fig. 4a). Subjects’ aggregate ratings of choice set value in task 3 showed the expected inverted U-shaped function of S (Fig. 1d). Any region that similarly exhibited an inverted

U-shaped neural activity as a function of S , approximated by the quadratic predictor, was considered a candidate area representing choice set value (Fig. 4). Going further, based on behavioural evidence¹¹, we tested whether those regions with an inverted U-shaped activity profile also showed (1) increased value for less complex processing (CF > NF) and (2) diminished quadratic activity if the costs of choosing are removed in FO trials. Regions within the left dorsal striatum, namely the caudate nucleus (CN) and the putamen, as well as the right ACC, did exhibit an inverted U-shaped activity profile as a function of choice set size S in free choice trials while also fulfilling the above two criteria (1) and (2) (Fig. 4). Importantly, the overall characteristic of the observed activity profiles, which correlates with choice set value, could neither be directly explained by differences in the stimulus material nor by the statistics of our choice sets (Supplementary Fig.1) or by any of the behavioural parameters that were assessed in our study (Fig. 3). In our Supplementary Discussion we further discuss various factors that, potentially, could have confounded our results. We conclude that explaining the overall pattern of activity in ACC and the dorsal striatum by choice set value is the most parsimonious interpretation of our data.

Earlier studies have shown that ACC contains neurons that reflect various decision variables such as reward probability, reward magnitude and physical decision costs. It was thought to also represent an integrated value signal that considers both these costs and benefits^{31,32}. In fact, electrophysiological recordings from ACC

neurons have demonstrated a representation of both the discounted value of chosen items and of decision costs such as physical effort or temporal delay³³. Accordingly, human ACC has representations of anticipated effort^{34,35}, and the effort-discounted value of reward offers in decision-making experiments^{36,37}. Similarly, our results revealed that the right ACC—as opposed to the left dorsal striatum—does exhibit signal components that linearly increase with choice set size *S* and that correlate with perceived choice difficulty (Supplementary Table 1). These signal components could reflect the cost of choosing from a particular choice set. On the other hand, the simultaneous presence of a quadratic signal component in ACC suggests that it also reflected the overall value of a choice set, net of decision costs. As opposed to previous experiments, however, these putative cost and net value signals in ACC value the choice set as a whole. The idea that the ACC represents such a ‘global’ cost and value signals is also in agreement with a recent investigation that engaged a ‘human foraging paradigm’ where ACC reflected the average value of the (global) foraging environment as well as foraging costs³⁸. Finally, our findings are also compatible with the suggestion that integrated value signals in ACC ‘determine whether, where and how much control to allocate’²², consistent with the concept of choice set value as a driver of motivation and cognitive engagement.

As with activity in the right ACC, areas within the left dorsal striatum—the caudate nucleus and the putamen—also displayed quadratic activity patterns that appear to represent choice set value. Consistent with this interpretation, striatal areas have been shown previously to reflect subjective value signals³⁹ and to discount value information by cost factors such as anticipated physical effort^{21,35} or experienced cognitive demands⁴⁰. However, these studies have reported net value representations for the ventral striatum, whereas, here, we have uncovered set value related activity in dorsal striatum. The reason for this discrepancy could simply refer to the fact that our study entailed a choice task while the other studies did not require their subjects to choose. Yet, consistent with our findings, various studies have shown that activity within the dorsal striatum increases when subjects invest less effort^{21,36,41}. Moreover, in a comparable task design, researchers have shown that overlapping areas within the dorsal striatum exhibit fMRI activity that scales with expected reward and with subjects’ motivation^{42–44}. Hence, the reported activity profiles within the left dorsal striatum could resemble our subjects’ motivation to choose from a given set: they could reflect the increasing attractiveness of larger sets during ‘browsing’ and the set-attractiveness, discounted by the decision costs for larger sets, in the case of ‘choosing’ (Fig. 4b). In fact, the dorsal striatum is in an ideal anatomical position to propagate such set value related information to areas engaged in both cognitive control and motor behaviour^{45,46}. Similar to ACC, it could motivate engagement in executive control^{23,47,48} and enable decision making from multiple alternatives, as long as it does not get too costly. Conceptually, this operational interpretation of choice set value agrees well with the concept of ‘intensity of motivation’ of ref. 49. Based on a vast body of empirical work these authors suggest that ‘motivational arousal rises with increasing difficulty of instrumental behaviour up to the point where the required effort is greater than is justified by the motive, or the required effort surpasses the individual’s skills and abilities, at which point arousal drops to a low level’ (p. 129) (see, for example, ref. 50 for related empirical work). This description resembles our own explanatory model well (Fig. 1a) and thus, at least in the context of our study, ‘intensity of motivation’ and ‘choice set value’ could reflect two sides of the same coin.

The value of the choice set was not the only value signal that was present in the left dorsal striatum. In fact, the nature of the value representation within the striatum varied across the different stages of our task: while set value was exclusively encoded during the exposure stage of a trial, a representation of the value of the chosen item emerged at later task stages (Fig. 4e). This pattern further

suggests that representations of (1) the value of the set and (2) the value of the chosen item are distinct and temporally separable. One may further conclude that the decision costs experienced during the process of choosing have no impact on the value signal for the chosen item. Our overall findings therefore confirm and significantly extend previous conceptions of value coding in dorsal striatum.

Besides the dorsal striatum, the left orbitofrontal (POG) and left dorsolateral prefrontal cortex (MFG) also appear to reflect choice set value. Both areas exhibited an inverted U-shaped activity profile in choice trials (CF and NF), but there were only weaker trends to changes in activity in those areas based on choice complexity and decision intent (Supplementary Fig. 3). The representation of choice set value in these areas could be explained by their recruitment through motivational signals from the striatum or ACC: the orbitofrontal cortex (POG) could be engaged in representing the ‘space of goods’ in our task and in choosing between the individual items⁵¹. The MFG is typically thought to play a crucial role in cognitive control, attention and working memory^{52–55}. We can therefore speculate that lower fMRI activity in MFG in response to the largest choice sets might indicate a reduction of sustained cognitive control, or ‘mental fatigue’, in the face of choice overload⁵⁶.

The major contribution of our study is to demonstrate the neural substrates that reflect the integrated costs and overall net benefits of choosing from sets with multiple alternatives, namely the dorsal striatum and the ACC. Another important, though unexpected, outcome of our study was that such representations of set value and of the value of the chosen item are represented in a temporally distinct fashion. This has important theoretical and practical implications, as it suggests that the costs of choosing only enter into the value of the set, and not into the value of the chosen item. Further research is needed, however, to more precisely detail the actual roles and the interplay of all task-related areas in the process of choosing from multiple alternatives as well as their time course.

Looking forward, it would be desirable to devise experiments that are able to identify representations of specific costs and benefits and to uncover how they contribute to set value representations (for example, by means of establishing functional connectivity between representations of the net value of a set and other areas processing specific costs and benefits⁴⁰). This could help to define the true nature and origin of those costs and benefits, which are difficult to uncover when using solely behavioural studies or self-reports. The latter is particularly true for isolating the costs of neural processing, which, metabolically, are the most expensive³⁷. Hence, based on brain-imaging data, new insights into various types of cost and benefit can be revealed and the temporary influence of these factors on set value versus chosen value can be identified. In cases where it is difficult to accurately predict the value of choice sets purely from behavioural comparisons or subjective reports, neural data could conceivably improve prediction^{58,59}.

Importantly, although these insights are necessarily based on correlational analytical techniques, identification of the neural circuitry of choice overload invites causal experiments that can critically probe the developed models using non-invasive brain stimulation (for example, using transcranial magnetic stimulation (TMS) or transcranial direct current stimulation (tDCS) to increase or decrease particular cost–benefit calculations) or through lesion patient studies. This will help to further detail psychological and economic models of choice overload and to find the actual ‘bottle-necks’ that delimit our ability to choose easily from multiple alternatives.

Knowing more about choice overload, and ideal choice set sizes, can be important for informing public policy. Governments and organizations often must decide how many options to give to citizens, employees or customers in important decisions such as the choice of a pension scheme, a health plan or a medical option such as elective surgery. Knowledge of the origins of costs and benefits

associated with the overall array of options could enable governments to help citizens make better active decisions without appreciably restricting freedom^{60,61}.

This study only tested variation of choice overload with two features: complexity (CF versus NF) and decision intent (choosing in NF versus browsing in FO). Further research should address the effect and neural representation of other moderators of choice overload. Promising variables include time pressure, possible differences between cultures (because autonomous, personal choice is more strongly valued in some cultures than in others^{62,63}) and individual differences due to expertise¹⁰ or personality traits.

Given our results, it would be especially interesting to know whether neural activity in dorsal striatum and ACC might account for inter-individual differences in perceived set value. For example, one would expect that for people who report stronger choice overload in their amount ratings (Fig. 1c), the neural activity should also exhibit a stronger inverted U-shaped pattern than for subjects experiencing less choice overload. Moreover, this difference should be particularly apparent in the more difficult NF condition. Instead, we would expect the neural activity in set value related areas to become more linear when a clear favourite alternative, alleviating choice overload, is present. While our study was not designed to show such interrelations (Supplementary Discussion), we offer some preliminary results on inter-individual differences (Supplementary Fig. 4). In brief, based on the individual amount ratings of sets (Fig. 1c), subjects were divided into two groups: subjects showing a weaker sensitivity of the amount rating to *S* were assigned to the 'low slope' group and those with higher sensitivity to the 'high slope' group. The two groups did not differ in any of the other behavioural measures obtained. As expected¹⁰, the neural activity profile was more steeply quadratic in the high slope group in the NF condition. Consistent with our prediction, the activity in CF changed from a quadratic to a linear profile in the high slope group. Surprisingly, however, the low slope group maintained the inverted U-shaped activity profile in both free choice conditions. These preliminary results highlight discrepancies between the subjective experience of choice (which differs across groups) and objective choice performance (which is similar), and highlight the potential use of neural measurement as an objective means that could capture this explanatory gap⁴² and that could provide new and stimulating insights.

Our results are also relevant to an emerging value-and-compare view in decision neuroscience, in which choices are made by valuing all the objects in a choice set, then comparing them and choosing the best one⁶⁴. Evidence that supports this view includes a wide range of data from neural firing rates accompanying binary choices of monkeys⁵¹ to fMRI responses in humans expressing values of many types of goods with multiple dimensions⁶⁵. However, most of these studies have used a small number of choices (typically 2–3). Such small choice sets cannot be used to identify U-shaped value components, and are too limited to separate decision costs, item valuation and choice set valuation. A complete neuroeconomic account of choice could emerge by synthesizing evidence for the value-and-compare model with heuristic approaches when there are many choices, accounting for how choice difficulty enters when people choose from multiple items or among sets of choices.

In summary, we have demonstrated that activity in left dorsal striatum and right ACC reflects choice set value and could serve as a neural indicator of choice overload. Moreover, we suggest that these areas integrate costs and benefits of choice sets to motivate the recruitment of cognitive and behavioural resources during decision making. More research is certainly needed to reveal when and why there are too many alternatives, and for specifying how different contextual and personal variables contribute to the quality and experience of choice.

Methods

Subjects. Nineteen individuals (12 males; age (mean \pm s.d.) 26.2 \pm 4.9 years) completed the study. All subjects were right-handed and had normal or corrected to normal vision. Participants signed the informed consent form before participating in the experiment. The study was performed in accordance with the Caltech Institutional Review Board guidelines. Initially we recruited 20 subjects. One subject reported verbally that he was indifferent about landscape images, was not interested in choosing any of them, and even rejected the customized item as a reward at the end of the experiment. His ratings of the landscape images indicated the same: there was no variability in the liking ratings of different images that he reported. Over 84% of images were given a rating of '0' (meaning that the subject did not like the images at all), and the remaining 16% of ratings were distributed between 0 and 1.8 on the 11-point scale ($M = 0.1$, s.d. = 0.28). The data clearly indicated that the task was not engaging for that particular subject. Therefore, the data from that subject were not included in further analysis (behavioural or fMRI). Sample size was guided by a previous behavioural study on choice overload¹³ and built on a power-analysis ($\alpha = 0.05$, power = 0.8) (see Supplementary Methods for details).

Experimental procedures. Further experimental procedures are provided in the Supplementary Methods.

fMRI. A 3 T Siemens TRIO scanner and an eight-channel head coil (Siemens) were used to acquire MRI images. A T1-weighted MP-RAGE anatomical scan (176 slices, slice thickness = 1 mm, gap = 0 mm, in-plane voxel size = 1 \times 1 mm, repetition time (TR) = 1,500 ms, echo time (TE) = 3.05 ms, field of view (FOV) = 256 \times 256, resolution = 256 \times 256) as well as T2*-weighted gradient-echo planar imaging scans (EPIs: slice thickness = 3.5 mm, gap = 0 mm, in-plane voxel size = 3 \times 3 mm, TR = 2,000 ms, TE = 30 ms, flip angle = 90°, FOV = 192 \times 192, resolution = 64 \times 64, 32 axial slices) were obtained for each subject. In total, 1,512 EPIs per subject were collected during four consecutive runs lasting 13 min each.

We used SPM 5 (Wellcome Department of Cognitive Neurology, London) to perform functional image analyses. First, all images of each subject were realigned to the first scan of the first run. Next, we co-registered the mean image of the realigned functional scans to the anatomical image. The latter was then normalized to the SPM T1-template in Montreal Neurological Institute (MNI) space (mean brain). The resulting nonlinear 3D transformation was applied to all EPI images. Finally, we spatially smoothed the normalized functional images using a Gaussian kernel (7 \times 7 \times 7 mm³ full-width at half-maximum), then applied a high-pass filter (cutoff period 128 ms). Note, that we did not perform slice-time correction because scans were acquired in an interleaved fashion.

Subsequent fMRI analyses were first performed at the individual and then at the group level (note that we used the canonical analytical approach in SPM 5, which assumes normality; only for our behavioural performance measures was the assumption of normality confirmed statistically; see 'Statistical analyses' section in Supplementary Methods). On the individual level we used two different models. In model (1), nine experimental conditions were modelled separately (3 tasks (CF, NF and FO choice) \times 3 task stages (exposure and mask, delay, and response periods)) in the GLMs for a given subject. Each model also included six motion correction parameters obtained from a rigid-body transformation during image realignment, as well as three further parameters that served as additional parametric modulators for each of the 3 \times 3 condition-by-stage regressors of the GLMs: (1) a linear predictor, (2) a quadratic predictor (orthogonalized to the linear term) and (3) the liking rating of the chosen item. Parametric modulators are explained in more detail in the main text. Thus, there were a total of 6 motion regressors and 27 parametrically modulated condition-by-stage regressors (3 \times 3 \times 3 = 3 tasks \times 3 task stages \times 3 parametric modulators). To analyse model (1) at the group level, we restricted our calculations to task-related areas (across-subject activity increases in the exposure phase in either of the choice conditions, CF or NF, at $P < 0.01$ uncorrected (one-tailed *t*-test; null hypothesis (H_0): $\mu > 0$)). Then, contrast images for the various regressors of the exposure phase were analysed using one-tailed *t*-tests, allowing us to map brain regions that displayed an activity pattern in the pooled choice conditions NF and CF that was positively correlated with the quadratic predictor (H_0 : $\mu > 0$; $P < 0.05$ false discovery rate (FDR)-corrected for multiple comparisons) or with the linear predictor ($P < 0.01$ uncorrected; note that this liberal threshold was chosen to ensure high sensitivity for detecting any additional presence of a positive linear signal component in quadratic areas). Areas revealed by the latter contrast were considered potential candidates for being a neural correlate of choice set value. The beta estimates revealed for these areas were further subjected to ROI analyses (see below).

In model (2) the individual subjects' GLMs included regressors for each of our 3 \times 3 experimental conditions (3 tasks (CF, NF and FO choices) \times 3 choice sets *S* (6-, 12- and 24-item sets)) and for each stage of the task (exposure and mask, delay, and response period), amounting to 27 regressors per session. As in model (1), the six motion correction parameters obtained from the rigid-body transformations during realignment were included as additional regressors to capture any residual movement artefacts. The respective beta estimates, which were assessed by model (2), were subjected to additional ROI analyses (see below).

We also performed an explanatory group analysis in which we searched for voxels of task-related areas that would exhibit a positive linear correlation between the beta estimates of the pooled free choice conditions of the exposure phase and individual estimates of choice set value. However, this analysis did not reveal any significant result (threshold criterion: $P < 0.05$ FDR-corrected for multiple comparisons (one-tailed t -test; $H_0: \mu > 0$). In the Supplementary Discussion we discuss this null result, along with the suitability of alternative analytical and experimental approaches to assess neural correlates of choice set value.

ROI analyses. We used the SPM2 Volumes Toolbox v1.21 (Volkmar Glauche) to extract the normalized beta weights for the exposure period regressors of both model (1) and model (2) for a 3-mm-radius sphere that was centred on our functionally defined ROIs (see above).

We subjected the normalized beta weights revealed by model (1) to several analyses. First, we probed for the presence of a significant linear signal increase in the fMRI activity estimates of the exposure stage in the pooled choice conditions (CF and NF; one-tailed t -tests; $H_0: \mu > 0$). A paired t -test was performed on the beta estimates capturing the quadratic signal component in NF versus FO to probe for reductions of this signal component due to diminished decision costs in FO (paired t -test; $H_0: \mu_{FO} < \mu_{NF}$; Supplementary Table 1). Finally, we performed a two-way repeated measures ANOVA with the factors task stage (exposure, delay, response) and predictor (quadratic predictor versus value of the chosen item) on the beta values of our main ROIs (Fig. 4e and Supplementary Fig. 3d). This analysis was exclusively performed to reveal any potential interaction between the two factors, namely a temporally distinct representation of set value (quadratic predictor) and the value of the chosen item. We did not consider a main effect of the factor 'predictor' as the respective beta estimates between the two GLM predictors are not directly comparable (due to the varying range of the respective parametric modulators). In addition, we performed one-tailed t -tests on these beta estimates for each respective factor combination (regressor \times task stage) to probe for any positive correlation of these regressors with the fMRI signal ($H_0: \mu > 0$; Supplementary Table 2).

The normalized beta weights of model 2 were subjected to a regression analysis in which we correlated the beta weights of the pooled choice conditions (CF and NF) for the exposure stage with (1) the number of saccades and (2) subjects' difficulty ratings (Supplementary Table 1). We also performed a two-way repeated measures ANOVA with the factors condition (CF versus NF) and set size (S ; effect of no interest) on these beta estimates to exhibit signal changes due to the availability of a dominant option (in CF but not in NF) (Supplementary Table 1).

Reporting Summary. Further information on research design is available in the Nature Research Reporting Summary linked to this article.

Code availability. In this study we utilized standard software and published analytical routines, as specified in detail in the Methods and in the Supplementary Methods. Related Matlab code is available from the corresponding author upon reasonable request. All landscape images were obtained from www.terrageria.com with the permission of the author and cannot be made available with our stimulus code.

Data availability

The data that support the findings of this study as well as the data underlying our power calculations are available from the corresponding author upon reasonable request. Unthresholded statistical maps of our main fMRI-results are available at NeuroVault.org⁶⁶ (<https://neurovault.org/collections/4117/>).

Received: 22 January 2017; Accepted: 23 August 2018;

Published online: 01 October 2018

References

- Schwartz, B. & Ward, A. in *Positive Psychology in Practice* (eds Linley, P. A. & Joseph, S.) Ch. 6 (Wiley, New York, 2004).
- Iyengar, S. S., Huberman, G. & Jiang, W. *Pension Design and Structure: New Lessons from Behavioral Finance* (eds Mitchell O. S. & Utkus S. P.) Ch. 5 (Oxford Scholarship Online, Oxford, 2004).
- Iyengar, S. S. & Lepper, M. R. When choice is demotivating: can one desire too much of a good thing? *J. Pers. Soc. Psychol.* **79**, 995–1006 (2000).
- Steiner, I. D. Perceived freedom. *Adv. Exp. Social Psychol.* **5**, 187–248 (1970).
- Reibstein, D. J., Youngblood, S. A. & Fromkin, H. L. Number of choices and perceived decision freedom as a determinant of satisfaction and consumer behavior. *J. Appl. Psychol.* **60**, 434–437 (1975).
- Zuckerman, M., Porac, J. F., Lathin, D., Smith, R. & Deci, E. L. On the importance of self-determination for intrinsically motivated behavior. *Pers. Soc. Psychol. Bull.* **4**, 443–446 (1978).
- Ryan, R. M. & Deci, E. L. Self-determination theory and the facilitation of intrinsic motivation, social development, and well-being. *Am. Psychol.* **55**, 68–78 (2000).
- Sarver, T. Anticipating regret: why fewer options may be better. *Econometrica.* **76**, 263–305 (2008).
- Loewenstein, G. Is more choice always better? *Social Security Brief* **7**, 1–8 (1999).
- Chernev, A. When more is less and less is more: the role of ideal point availability and assortment in consumer choice. *J. Consum. Res.* **30**, 170–183 (2003).
- Chernev, A., Böckenholt, U. & Goodman, J. Choice overload: a conceptual review and meta-analysis. *J. Consum. Psychol.* **25**, 333–358 (2015).
- Shah, A. M. & Wolford, G. Buying behavior as a function of parametric variation of number of choices. *Psychol. Sci.* **18**, 369–370 (2007).
- Reutsjkaja, E. & Hogarth, R. M. Satisfaction in choice as a function of the number of alternatives: when 'goods satiate'. *Psychol. Market.* **26**, 197–203 (2009).
- Schwartz, B. & Grant, A. M. Too much of a good thing: the challenge and opportunity of the inverted-U. *Persp. Psychol. Sci.* **6**, 61–76 (2011).
- Reutsjkaja, E., Camerer, C., Nagel, R. & Rangel, A. Search dynamics in consumer choice under time pressure: an eye-tracking study. *Am. Econ. Rev.* **101**, 900–926 (2011).
- Coombs, C. H. & Avrunin, G. S. Single-peaked functions and the theory of preference. *Psychol. Rev.* **84**, 216–230 (1977).
- Scheibehenne, B., Greifeneder, R. & Todd, P. M. Can there ever be too many options? A meta-analytic review of choice overload. *J. Consum. Res.* **37**, 409–425 (2010).
- Chernev, A. Decision focus and consumer choice among assortments. *J. Consum. Res.* **33**, 50–59 (2006).
- Chernev, A. & Hamilton, R. Assortment size and option attractiveness in consumer choice among retailers. *J. Marketing Res.* **46**, 410–420 (2009).
- Choi, J. & Fishbach, A. Choice as an end versus a means. *J. Marketing Res.* **48**, 544–554 (2011).
- Crosson, P. L., Walton, M. E., O'Reilly, J. X., Behrens, T. E. J. & Rushworth, M. F. S. Effort-based cost-benefit valuation and the human brain. *J. Neurosci.* **29**, 4531–4541 (2009).
- Shenhav, A., Botvinick, M. M. & Cohen, J. D. The expected value of control: an integrative theory of anterior cingulate cortex function. *Neuron* **79**, 217–240 (2013).
- Botvinick, M. & Braver, T. Motivation and cognitive control: from behavior to neural mechanism. *Annu. Rev. Psychol.* **66**, 83–113 (2015).
- Andersen, R. A. & Buneo, C. A. Intentional maps in posterior parietal cortex. *Annu. Rev. Neurosci.* **25**, 189–220 (2002).
- Grill-Spector, K. & Malach, R. The human visual cortex. *Annu. Rev. Neurosci.* **27**, 649–677 (2004).
- Orban, G. A., Van Essen, D. & Vanduffel, W. Comparative mapping of higher visual areas in monkeys and humans. *Trends Cogn. Sci.* **8**, 315–324 (2004).
- Medendorp, W., Beurze, S., Van Pelt, S. & Van Der Werf, J. Behavioral and cortical mechanisms for spatial coding and action planning. *Cortex* **44**, 587–597 (2008).
- Lindner, A., Iyer, A., Kagan, I. & Andersen, R. A. Human posterior parietal cortex plans where to reach and what to avoid. *J. Neurosci.* **30**, 11715–11725 (2010).
- Rosenbaum, D. A. Human movement initiation: specification of arm, direction, and extent. *J. Exp. Psychol. Gen.* **109**, 444–474 (1980).
- Kimmig, H. et al. Relationship between saccadic eye movements and cortical activity as measured by fMRI: quantitative and qualitative aspects. *Exp. Brain Res.* **141**, 184–194 (2001).
- Kennerley, S. W., Dahmubed, A. F., Lara, A. H. & Wallis, J. D. Neurons in the frontal lobe encode the value of multiple decision variables. *J. Cogn. Neurosci.* **21**, 1162–1178 (2009).
- Rushworth, M. F. S. & Behrens, T. E. J. Choice, uncertainty, and value in prefrontal and cingulate cortex. *Nat. Neurosci.* **11**, 389–397 (2008).
- Hosokawa, T., Kennerley, S. W., Sloan, J. & Wallis, J. D. Single-neuron mechanisms underlying cost-benefit analysis in frontal cortex. *J. Neurosci.* **33**, 17385–17397 (2013).
- Prévost, C., Pessiglione, M., Méteureau, E., Cléry-Melin, M. L. & Dreher, J. C. Separate valuation subsystems for delay and effort decision costs. *J. Neurosci.* **30**, 14080–14090 (2010).
- Kurniawan, I. T., Guitart-Masip, M., Dayan, P. & Dolan, R. J. Effort and valuation in the brain: the effects of anticipation and execution. *J. Neurosci.* **33**, 6160–6169 (2013).
- Klein-Flügge, M. C., Kennerley, S. W., Friston, K. & Bestmann, S. Neural signatures of value comparison in human cingulate cortex during decisions requiring an effort-reward trade-off. *J. Neurosci.* **36**, 10002–10015 (2016).
- Chong, T. T. et al. Neurocomputational mechanisms underlying subjective valuation of effort costs. *PLoS Biol.* **15**, e1002598 (2017).
- Kolling, N., Behrens, T. E., Mars, R. B. & Rushworth, M. F. Neural mechanisms of foraging. *Science* **336**, 95–98 (2012).
- Schultz, W. Reward functions of the basal ganglia. *J. Neural Transm.* **123**, 679–693 (2016).

40. Botvinick, M. M., Huffstetler, S. & McGuire, J. T. Effort discounting in human nucleus accumbens. *Cogn. Affect. Behav. Neurosci.* **9**, 16–27 (2009).
41. Kurniawan, I. T. et al. Choosing to make an effort: the role of striatum in signaling physical effort of a chosen action. *J. Neurophysiol.* **104**, 313–321 (2010).
42. Iyer, A., Lindner, A., Kagan, I. & Andersen, R. A. Motor preparatory activity in posterior parietal cortex is modulated by subjective absolute value. *PLoS Biol.* **8**, e1000444 (2010).
43. Apicella, P., Ljungberg, T., Scarnati, E. & Schultz, W. Responses to reward in monkey dorsal and ventral striatum. *Exp. Brain Res.* **85**, 491–500 (1991).
44. Samejima, K., Ueda, Y., Doya, K. & Kimura, M. Representation of action-specific reward values in the striatum. *Science* **310**, 1337–1340 (2005).
45. Alexander, G. E., De Long, M. R. & Strick, P. L. Parallel organization of functionally segregated circuits linking basal ganglia and cortex. *Annu. Rev. Neurosci.* **9**, 357–381 (1986).
46. Haber, S. N. Corticostriatal circuitry. *Dialogues Clin. Neurosci.* **18**, 7–21 (2016).
47. Schmidt, L., Lebreton, M., Cléry-Melin, M. L., Daunizeau, J. & Pessiglione, M. Neural mechanisms underlying motivation of mental versus physical effort. *PLoS Biol.* **10**, e1001266 (2012).
48. Schoupe, N., Demanet, J., Boehler, C. N., Ridderinkhof, K. R. & Notebaert, W. The role of the striatum in effort-based decision-making in the absence of reward. *J. Neurosci.* **34**, 2148–2154 (2014).
49. Brehm, J. W. & Self, E. A. The intensity of motivation. *Annu. Rev. Psychol.* **40**, 109–131 (1989).
50. La Gory, J., Dearen, B. B., Tebo, K. & Wright, R. A. Reported fatigue, difficulty, and cardiovascular response to an auditory mental arithmetic challenge. *Int. J. Psychophysiol.* **81**, 91–98 (2011).
51. Padoa-Schioppa, C. Neurobiology of economic choice: a good-based model. *Annu. Rev. Neurosci.* **34**, 333–359 (2011).
52. Cohen, J. D. et al. Temporal dynamics of brain activation during a working memory task. *Nature* **386**, 604–608 (1997).
53. Fletcher, P. C., Shallice, T. & Dolan, R. J. The functional roles of prefrontal cortex in episodic memory. I. Encoding. *Brain* **121**, 1239–1248 (1998).
54. Bechara, A., Damasio, H., Tranel, D. & Anderson, S. W. Dissociation of working memory from decision making within the human prefrontal cortex. *J. Neurosci.* **18**, 428–437 (1998).
55. MacDonald, A. W. III, Cohen, J. D., Stenger, V. A. & Carter, C. S. Dissociating the role of dorsolateral prefrontal and anterior cingulate cortex in cognitive control. *Science* **288**, 1835–1838 (2000).
56. Boksem, M. A. S. & Tops, M. Mental fatigue: costs and benefits. *Brain Res. Rev.* **59**, 125–139 (2008).
57. Attwell, D. & Laughlin, S. B. An energy budget for signaling in the grey matter of the brain. *J. Cereb. Blood Flow Metab.* **21**, 1133–1145 (2001).
58. Falk, E. B., Elliot, T. B. & Matthew, D. L. From neural responses to population behavior: neural focus group predicts population-level media effects. *Psychol. Sci.* **23**, 439–445 (2012).
59. Genevsky, A., Yoon, C. & Knutson, B. When brain beats behavior: neuroforecasting crowdfunding outcomes. *J. Neurosci.* **37**, 8625–8634 (2017).
60. Camerer, C. F., Issacharoff, S., Loewenstein, G., O'Donoghue, T. & Rabin, M. Regulation for conservatives: behavioral economics and the case for 'asymmetric paternalism'. *Univ. PA Law Rev.* **151**, 1211–1254 (2003).
61. Thaler, R. H. & Sunstein, C. R. *Nudge: Improving Decisions About Health, Wealth, and Happiness* (Penguin, London, 2009).
62. Iyengar, S. S. & Lepper, M. R. Rethinking the value of choice: a cultural perspective on intrinsic motivation. *J. Pers. Soc. Psychol.* **76**, 349–366 (1999).
63. Markus, H. R. & Schwartz, B. Does choice mean freedom and well-being? *J. Consum. Res.* **37**, 344–355 (2010).
64. Glimcher, P. W. in *Neuroeconomics: Decision Making and the Brain* (eds Glimcher, P. W., Camerer, C. F., Fehr, E. & Poldrack, R. A.) Ch. 32 (Academic Press, London, 2008).
65. Hare, T. A., Camerer, C. F. & Rangel, A. Self-control in decision-making involves modulation of the vmPFC valuation system. *Science* **324**, 646–648 (2009).
66. Gorgolewski, K. J. et al. NeuroVault.org: a web-based repository for collecting and sharing unthresholded statistical maps of the brain. *Front. Neuroinform.* **9**, 8 (2015).
67. Masson, M. E. & Loftus, G. R. Using confidence intervals for graphically based data interpretation. *Can. J. Exp. Psychol.* **57**, 203–220 (2003).

Acknowledgements

The authors acknowledge support from the Spanish Ministry of Science and Education, grants nos. ECO2011-29865 (to E.R.), SEJ2005-08391 and ECO2008-01768 (to R.N.), the German Research Council (DFG CIN) (to A.L.), Generalitat de Catalunya, and BGSE (to R.N.), the Moore Foundation (to C.F.C. and R.A.A.), the Human Frontier Science Program (to C.F.C., R.N. and E.R.), the National Institutes of Health (Conte to C.F.C. and R.A.A.), the National Science Foundation and Boswell Foundation (to R.A.A.), Caltech T&C Chen Social and Decision Neuroscience Center (to C.F.C.) and Caltech T&C Chen Brain–Machine Interface Center (to R.A.A.). The funders had no role in the conceptualization, design, data collection, analysis, decision to publish or preparation of the manuscript. The authors thank K. Quinn, A. Tank and A. Miro for help on previous versions of the manuscript.

Author contributions

Design was carried out by E.R., R.N., A.L., C.F.C. and R.A.A., fMRI collection by A.L. and E.R., fMRI analysis by A.L. and E.R. and other data analysis by E.R., A.L. and R.N. All authors contributed to writing the manuscript.

Competing interests

The authors declare no competing interests.

Additional information

Supplementary information is available for this paper at <https://doi.org/10.1038/s41562-018-0440-2>.

Reprints and permissions information is available at www.nature.com/reprints.

Correspondence and requests for materials should be addressed to A.L.

Publisher's note: Springer Nature remains neutral with regard to jurisdictional claims in published maps and institutional affiliations.

© The Author(s), under exclusive licence to Springer Nature Limited 2018